Adsorption (2012) 18:239–249
DOI 10.1007/s10450-012-9397-z

Hydrogen adsorption on microporous materials at ambient temperatures and pressures up to 50 MPa

Tyler G. Voskuilen · Timothée L. Pourpoint · Anne M. Dailly

Received: 3 February 2012 / Accepted: 6 August 2012 / Published online: 23 August 2012

Abstract High surface area microporous adsorbents are often proposed as potential hydrogen storage materials, although typically at 77 K and less than 5 MPa. In this study, we focus on conditions more suitable for automotive applications by investigating the storage capacities of microporous materials at 298 K and at pressures up to 50 MPa. In an effort to derive trends within and across material classes, we examined a wide range of materials with varying microstructures including the activated carbons AX-21, KUA-5, and MSC-30; a zeolite templated carbon; a hypercrosslinked polymer; and the Metal Organic Frameworks MOF-177, IRMOF-20, MIL-53, ZIF-8, and $Cu_3(btc)_2$. The peak excess adsorption of these materials ranged from 0.8–1.8 wt.%, although many did not reach their maximum capacity even at high pressures. However, the total volumetric storage gains over compressed hydrogen gas were quite low and, in many cases, negative. In addressing ambient temperature adsorption at significantly higher pressures than previously reported, our data confirms and extends the range of validity of several existing DFT calculations. Furthermore, our data suggest that, for both activated carbons and MOFs, factors other than specific surface area govern ambient temperature adsorption capacity. Contrary to some reports, the high fractions of sub-nanometer pores in some of the investigated MOFs did not appear to enhance the excess adsorption even at high pressures. For on-board applications with ambient temperature storage, significant enhancements to the attractive force at the materials' surface are required, beyond merely increasing specific surface area, or for MOFs, tuning of pore sizes.

Keywords Hydrogen storage · Adsorption · Zeolite templated carbon · Metal organic framework · Activated carbon

T.G. Voskuilen
School of Mechanical Engineering, Purdue University, West Lafayette, IN 47906, USA

T.L. Pourpoint (✉)
School of Aeronautics and Astronautics, Purdue University, West Lafayette, IN 47906, USA
e-mail: timothee@purdue.edu

A.M. Dailly
General Motors Global R&D Center, Warren, MI, USA

1 Introduction

Microporous adsorbents are one of the major classes of materials studied for gas storage. In particular, interest in on-board hydrogen storage applications has prompted extensive studies of such materials due to their high gravimetric hydrogen capacities at 77 K and relatively low pressures (less than 5 MPa). Primarily these studies have focused on activated carbons and metal organic frameworks (MOFs) as the most promising classes of materials. Recent studies at ambient temperature have reported gravimetric capacities of around 1.5 to 2 wt.% at pressures ranging from 30 to 70 MPa for a variety of activated carbons including AX-21, MSC-30, KUA1, and KUA5, as well as on structured materials such as zeolite-templated carbons (Jordá-Beneyto et al. 2007; Nishihara et al. 2009; Casa-Lillo et al. 2002). However, such measurements on MOFs under high pressures have not been reported in the open literature. In this work we examine the storage properties of activated carbons and MOFs at ambient temperature (298 K) and up to 50 MPa. Our goals are to (1) determine whether the well-controlled microstructure of the MOF can be used to increase its capacity at high pressures beyond what has been observed on activated carbons

and (2) assess whether these materials can offer significant increases in volumetric storage capacities relative to compressed hydrogen gas.

Several authors have modeled the limits of physisorption on carbon in slit-like pores at ambient temperature. Alcañiz-Monge et al. calculated a theoretical maximum excess adsorption of 3.5 wt.% for microporous activated carbon at ambient temperature (2008). Züttel et al. calculated a theoretical maximum uptake of 3.3 wt.% for hydrogen on single-walled carbon nanotubes (2002). In contrast, measured capacities of such materials at ambient temperature have been limited to the range of 1.5 to 2 wt.%. The difference between the measured capacities and the calculated upper limits suggest that the structure of activated carbons and other carbon structures could be tailored to increase their adsorption capacity at ambient temperature. However, as pointed out by Nishihara et al., the processes used to increase surface area in activated carbons are typically detrimental to the material's micropore volume (2009). Both of these properties, surface area and micropore volume, are typically regarded as indicators of a material's potential capacity, so this trade-off may or may not result in lower total adsorption.

Metal organic frameworks (MOFs) are crystallographically well-defined structures that are assembled by the connection of secondary building units (SBUs), usually consisting of metal ions or clusters, through rigid organic ligands. MOFs can be synthesized using a variety of bridging ligands and metal cation nodes, providing the ability to tune the nature and the size of the pores within the structures. This is one of the greatest advantages of MOFs over traditional adsorbents such as inorganic zeolites and porous activated carbons. The extent to which pore geometry and functionality affect the nature of the adsorbed hydrogen phase is a crucial question in determining if and how these materials can be improved. Additionally, recent published measurements of hydrogen adsorption on MOFs using neutron scattering and other techniques have demonstrated that the binding enthalpy on open metal sites in such MOFs can be greater than 10 kJ/mol, compared with the typical enthalpy of 4–6 kJ/mol for most adsorbents (Sumida et al. 2011; Krkljus and Hirscher 2011). In addition to changing the pore sizes, this offers another potential avenue for increasing the overall adsorption enthalpy on MOFs. While significant work has been done to establish the key physical properties that influence the hydrogen storage behavior of MOFs at cryogenic conditions, very little has been reported at ambient temperature and for pressures above 10 MPa. In fact, most ambient temperature adsorption measurements have been performed at pressures less than 15 MPa, where excess maximum uptake has not been reached and where the excess adsorption isotherm is linear with respect to pressure. Thus, extending these measurements for MOFs to pressures up to 50 MPa can provide useful insights about the mechanisms and limitations of hydrogen adsorption at ambient temperature (298 K).

Many previous publications have examined adsorbent materials in detail over temperatures ranging from 50 to 300 K at pressures up to 4–5 MPa (see, for example, Poirier and Dailly 2009; Schmitz et al. 2008). These measurements are often used with an appropriate adsorption model to determine the enthalpy of adsorption at different levels of surface coverage. While this enthalpy of adsorption provides a metric for evaluating a material's potential room temperature storage capacity and an indication of the strength of the interaction between the hydrogen and the adsorbate, extrapolating such models and fitted parameters several orders of magnitude beyond their original ranges does not in general provide accurate predictions of adsorption capacity. For example, Richard et al. (2009) fit the Dubinin-Astakhov model to data for adsorption on AX-21 available in the open literature at temperatures ranging from 77 to 300 K and pressures up to 5 MPa to determine the appropriate model parameters, including the adsorption enthalpy. However, since their model was fit only up to 5 MPa, if we extend it to 50 MPa it predicts an adsorption capacity (5 wt.%) which exceeds the theoretical limits mentioned previously for adsorption on carbons (Alcañiz Monge and Roman-Martinez 2008 and Züttel et al. 2002).

As demonstrated by many recent publications (Kumar et al. 2012; Chen et al. 2012; Gotzias et al. 2012; Xiong and Keffer 2011; Liu et al. 2009), detailed information about a material's crystallographic and atomic structure can be used in density functional theory and grand canonical Monte Carlo simulations to model both the heat of adsorption and the adsorbed phase density; however such work is typically still compared with experimental data taken at relatively low pressures (less than 10 MPa). As we will discuss in Sect. 3.2, such models can provide much better agreement with our high pressure measurements, however these models require detailed information about the material's atomic structure which is not readily determined from cryogenic isotherms.

2 Methods

A high pressure Sievert system was developed for hydrogen sorption measurements and detailed in a prior publication (Voskuilen et al. 2010). An overview of the system, details of the experimental procedures adapted to adsorbent materials, and data analysis methods are included herein.

2.1 High pressure Sievert system

The main components of the high pressure Sievert system used for these measurements, and of any volumetric adsorption instrument, are a reservoir volume and a sample

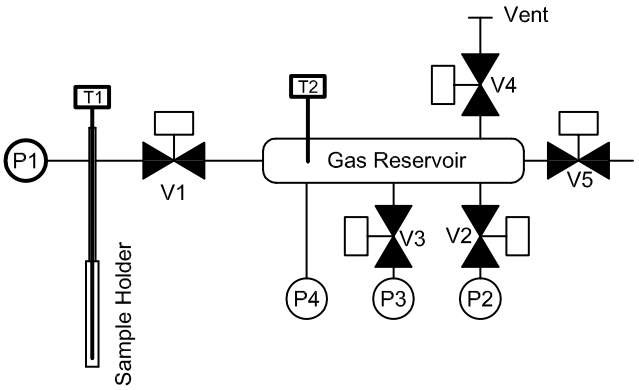

Fig. 1 High pressure Sievert system plumbing and instrumentation diagram, where pressure transducers, thermocouples, and pneumatic valves are noted by P, T, and V, respectively

chamber (shown in Fig. 1). The reservoir volume is well insulated from ambient to minimize spatial temperature gradients and damp out transient temperature variations, and is instrumented with a T-type thermocouple (±0.5 K) and three high accuracy pressure transducers (Druck PMP4060 series, 0.04 % FS total error) with different ranges (typically 7 MPa, 20 MPa, and 70 MPa, with a 2 MPa transducer available when needed). The lower pressure transducers can be isolated from the reservoir and the volume of the reservoir has been calibrated independently for each transducer configuration, since the volumes of the pressure transducer connections vary enough to affect the measurement's accuracy.

Temperature gradients throughout the system are measured by T type thermocouples attached to the exterior of the junction above the sample chamber and inside the sample holder and reservoir chamber. Sample holders of different volumes are available to allow measurements on samples down to about 200 mg. The required quantity of material in a volumetric apparatus is directly proportional to the total amount of hydrogen adsorbed, so materials with lower hydrogen uptake require larger samples to obtain measurements with the same level of accuracy.

2.2 Measurement procedures

All material handling, sample loading, and weighing were done in an inert argon atmosphere on a precision balance (±0.05 mg), then outgassed in the sample holder at 423 K and a vacuum of less than 10^{-3} Torr for at least 14 hours prior to any sorption measurements. The free volume inside the sample holder was determined by high purity helium expansion into the sample holder following each hydrogen adsorption test. Each material was tested multiple times to verify repeatability and consistency of measurement. Tests with no sample present in the sample chamber, or blank tests, were also performed before and after each set of tests to determine background adsorption, verify there were no leaks, and verify all volume calibrations. At the highest pressure point in each test, the system was held for 10–15 minutes and monitored for any pressure changes to verify leak-free operation. Finally, samples were re-weighed after testing to verify consistent sample mass before and after degassing and testing.

2.3 Data analysis

The measured excess adsorption was calculated using the measured pressures and temperatures in the system by determining the gas density changes in the reservoir volume and the sample chamber at each pressure step, and using the calibrated volumes to perform a hydrogen mass balance on the reservoir. The compressibility factors for hydrogen gas were used in all calculations based on the NIST database and the pressure and temperature measured in the system (Leachman et al. 2009). The total uncertainty in the measured adsorption was calculated using an independent random and bias error for each instrument, as well as the uncertainties in the system volumes. Further details about the relative effects of the various sources of uncertainty on the final measurements are included in the Appendix.

In this analysis, the effect of helium adsorption was assumed to be negligible and was not included in the calculations. The validity of this assumption and its potential effect on the measured values is discussed in the Appendix.

2.4 Material synthesis

A series of microporous materials of different types were evaluated as hydrogen adsorbents for ambient temperature and high pressure applications. The superactivated carbons AX-21 and MSC-30 were obtained from Anderson Development Company and Kansai Coke and Chemicals, respectively. The activated carbon KUA-5 was prepared from a Spanish anthracite by chemical activation with KOH as described by Lozanó-Castello et al. (2001). A carbon with well-defined micro-structure was synthesized using the nanocasting approach outlined by Nishihara et al. for their material noted P7(2)-H (2009). The resulting zeolite templated carbon (ZTC) was a structural replication from the hard template, Zeolite Y, from Tosoh Co. Ltd.

HCP is a developmental Hypercrosslinked Polymer material produced by Merck. A sample of HCP from a near-industrial scale batch of the material was used for this study.

Several MOFs composed of different inorganic clusters and linking organic units were investigated to compare the effects of different surface areas, pore size distributions, and metal cluster types. All laboratory scale samples were prepared via a one-pot reaction by solvothermal methods

from a solution or slurry of the metal ion salt with the corresponding linking organic unit. The activation of the porosity was achieved by the removal of non coordinating guests' species like solvent molecules in the pores and channels. MOF-177 is constructed from the BTB (4,4,4"-benzene-1,3,5-triyltribenzoate) and the basic zinc carboxylate cluster ($Zn_4O(CO_2R)_6$). IRMOF-20 is derived from the same high-symmetry SBU connected by TTDC (thieno[3,2-b]thiophene-2,5-dicarboxylate) linkers. $Cu_3(btc)_2$ combines the copper paddle wheel ($Cu_2(CO_2R)_4$) to the BTC (1, 3, 5-benzenetricarboxylate) ligand. MIL-53(Al) is built up from infinite chains of corner-sharing $AlO_4(OH)_2$ octahedra interconnected by BDC (1, 4-benzenedicarboxylate) units. Finally the zeolitic imidazolate framework ZIF-8 consisting of tetrahedral ZnN_4 clusters linked by MeIM (2-methylimidazolate) was considered.

2.5 Microstructure characterization

The porosimetry analysis of the studied materials was carried out via nitrogen and argon adsorption measurements at 77 K and 87 K, respectively, using a Quantachrome Autosorb-1 gas-sorption apparatus. The samples were degassed at 373 K under vacuum overnight prior to the experiments. The specific surface areas of the samples were calculated from N_2 adsorption data at 77 K over the $P.P_0^{-1} = 5 \times 10^{-2}$–$1.0 \times 10^{-1}$ range using the Brunauer-Emmett-Teller (BET) model (note that these conditions can influence the value of the calculated area). The total specific pore volumes were extracted from the saturation value of the argon adsorption isotherms measured at 87 K assuming liquid argon density. The pore size distribution was calculated using the density functional theory (DFT) applied over the argon adsorption data for all the samples except for ZTC whose pore size distribution was evaluated from nitrogen adsorption data.

3 Results and discussion

3.1 Microstructure properties

A summary of the structural properties of the evaluated materials is presented in Table 1. The skeletal densities included in the table were calculated from the difference between helium expansion at 1.5–2.0 MPa and room temperature in the sample holder containing the material and helium expansion in the empty sample holder, although they are not used in the determination of the excess isotherms. The evaluated skeletal densities are in decent agreement with the ones reported and published in the literature. The accuracy of the high pressure transducers leads to the relatively large error margin on the skeletal density results, but they remain appropriate and are included for comparison, taking into consideration the fact that the custom-made Sievert for high pressure sorption measurements is not the most accurate instrument for low pressure skeletal density measurements.

Table 1 Measured structural properties (BET specific surface area and specific porous volume), skeletal density and sample mass used for hydrogen testing of the studied adsorbents

Material	BET specific surface area ($m^2\,g^{-1}$)	Total specific pore volume ($cm^3\,g^{-1}$)	Skeletal density ($g\,cm^{-3}$)	Sample mass available for hydrogen sorption (g)
AX-21	2664	1.36	1.95 ± 0.1	0.972
KUA-5	2887	1.37	2.3 ± 0.5	0.572
MSC-30	3476	2.04	2.5 ± 0.5	0.500
ZTC	3035	2.21	1.9 ± 0.3	0.248
HCP	1762	2.34	1.3 ± 0.2	0.342
MOF-177	4126	1.67	1.5 ± 0.3	0.519
IRMOF-20	3689	1.67	1.6 ± 0.3	0.420
MIL-53	1286	0.64	1.4 ± 0.4	0.460
ZIF-8	1136	1.07	1.4 ± 0.4	0.551
$Cu_3(btc)_2$	1290	0.57	1.9 ± 0.3	1.260

MOF-177 and IRMOF-20 show high specific surface areas of 4126 and 3689 $m^2\,g^{-1}$, respectively, surpassing the activated carbons and ZTC specific surface areas, which are limited to about 3000 $m^2\,g^{-1}$. The other investigated MOFs and HCP show specific surface areas ranging from 1286 to 1762 $m^2\,g^{-1}$. Of the materials tested the MSC-30, ZTC, and hypercrosslinked polymer have the highest total pore volumes, while the MOFs with the smallest pores (MIL-53, ZIF-8, and $Cu_3(btc)_2$) predictably also have the smallest total pore volumes.

The pore volume distributions of the materials were measured in order to examine the potential relationship between specific ranges of pore sizes and room temperature hydrogen adsorption (Fig. 2). The activated carbons have a broad pore size distribution with a large amount of mesopores whereas the pore sizes in the ZTC are concentrated below 2 nm. The ZTC has a very sharp and intense peak around 1 nm which evidences the structural regularity and the effectiveness of the zeolite templating. In principle ZTCs have the same pore system that is replicated from the zeolite template structure but the porous texture highly depends on the synthesis conditions. The pores of the MOFs were much more narrowly distributed in the micropores range, as expected due to their highly ordered microstructures.

Of particular interest is the distribution of pores smaller than 1 nm. Prior theoretical and experimental work have suggested that pores smaller than 1 nm play a large role in ambient temperature adsorption due to the increased attractive force from multiple pore walls. The theoretical opti-

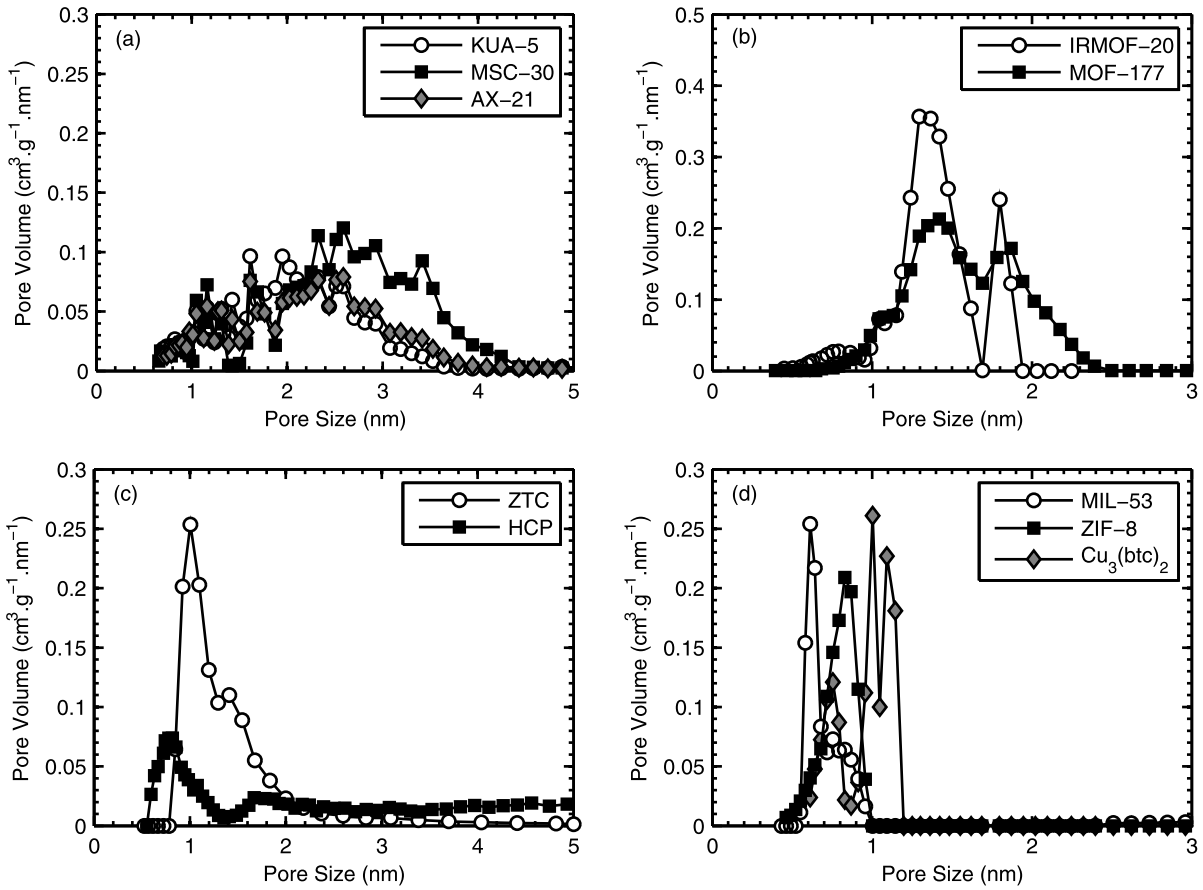

Fig. 2 Measured pore size distributions for (**a**) activated carbons, (**b**) MOF-177 and IRMOF-20, (**c**) zeolite templated carbon and hypercrossedlinked polymer, and (**d**) small pores based MOFs

mal pore size reported in the literature typically ranges from 0.6 nm to 0.9 nm (Alcañiz Monge and Roman-Martinez 2008; Im et al. 2008; Bhatia and Myers 2006; Gogotsi et al. 2009). Within this range, several authors have calculated that pores of around 0.9 nm are optimal for total storage over a range of pressures, due to their ability to hold multiple layers of adsorbate while maintaining relatively high attractive forces (Bhatia and Myers 2006; Wang and Johnson 1999). Looking at the fraction of pores smaller than 1 nm for all the materials, MIL-53 and ZIF-8 show the most potential in this regard solely based on their high volume fraction of pores smaller than 1 nm. However, their lower specific surface areas and lower total specific pore volumes may reduce their total storage capacity compared with some of the other MOFs and carbon structures.

3.2 Hydrogen excess adsorption at 298 K

The excess hydrogen uptakes measurements performed at 298 K and up to 50 MPa are presented in Fig. 3. Comparing the excess adsorption of the activated carbons with data available in the literature, the measured adsorbed quantities in this study are similar to the previously reported values and converge at around 1.2–1.5 wt.%. Unlike activated carbons we were not able to validate either the reported hydrogen capacity or the isotherm shape for the ZTC sample. The behavior of a ZTC reported in recent publication (Nishihara et al. 2009), a near linear isotherm, is indeed qualitatively different from activated carbons presenting curvature as they approach saturation. Our measured excess hydrogen isotherm for ZTC displays a similar level of curvature to the activated carbons rather than the linearly increasing capacity observed previously. The question remains whether the difference observed between our results and the reported data comes from the material synthesis or the hydrogen measurements. Even though the nitrogen adsorption isotherm, the specific surface area and micropore volume, the X-ray diffraction pattern obtained on our sample were nearly identical to the characterization data reported for P7(2)-H, we are aware that synthesis intricacies can lead to different properties.

For MOF-177, reported adsorption values at ambient temperature are limited to below 12 MPa in the open literature (Li and Yang 2007; Proch et al. 2008; Zacharia et al. 2010). The present measurements under 12 MPa compare

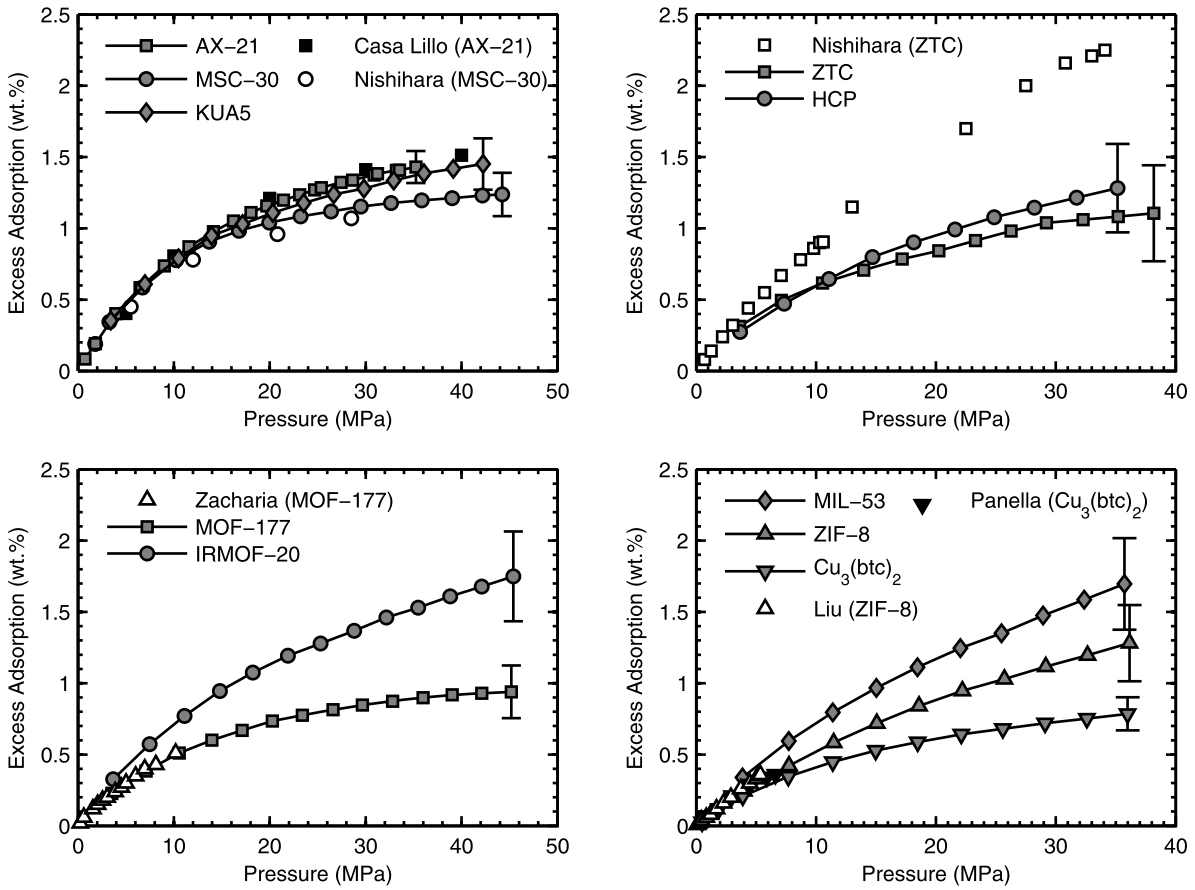

Fig. 3 Excess hydrogen adsorption at 298 K on various microporous adsorbents compared with some data from the literature where available (Casa-Lillo et al. 2002; Nishihara et al. 2009; Zacharia et al. 2010; Panella et al. 2006; Liu et al. 2009)

well with reported values, and extend the measurement up to 45 MPa. The present high pressure measurements reach a maximum of 0.94 wt.% at 45 MPa. This is an interesting result, since the sharp pore size distribution of MOF-177 suggests it might exhibit higher excess adsorption at 50 MPa than the activated carbons. In addition, the other bimodal pore Zn-based MOF, IRMOF-20, shows both a higher hydrogen uptake and a different isotherm shape and the excess uptake does not present similar curvature as the MOF-177 up to 45 MPa.

The excess hydrogen uptake measured on HCP at 298 K is very similar to those obtained on activated carbons even though HCP's specific surface area is two times lower than the surface areas of the activated carbons. This result suggests that the relationship between the specific surface area and the hydrogen sorption uptake observed at cryogenic conditions does not hold at room temperature (Kowalczyk et al. 2005; Wong-Foy et al. 2006). One possible contributing factor to this could be that the trend established at 77 K uses the maximum hydrogen uptake which is not always reached at the studied temperature and pressure. However, even considering only the materials which reached or closely approached saturation (the activated carbons and MOF-177) no distinct relationship is observed between BET specific surface area and hydrogen excess adsorption.

The lack of a trend between the specific surface area and excess adsorption at ambient temperature is also highlighted by the isotherms measured on ZIF-8, $Cu_3(btc)_2$ and MIL-53(Al). Excess adsorption measurements reported in the literature at ambient temperatures on these materials are also limited to pressures below 10 MPa (Li and Yang 2008; Panella et al. 2006; Liu et al. 2009). While these three MOFs have similar specific surface areas, the measured excess hydrogen uptakes are very different from one sample to another. MIL-53(Al) has the highest excess hydrogen uptake at 35 MPa, at about 1.7 wt.%, while $Cu_3(btc)_2$ does not exceed 1 wt.%. These three MOFs, while they have significantly lower surface areas than MOF-177 and IRMOF-20, exhibit similar magnitudes of adsorption, suggesting again that factors other than specific surface area govern ambient temperature adsorption capacity.

The measured surface density of hydrogen on ZIF-8, assuming a single adsorbed monolayer, is quite comparable to

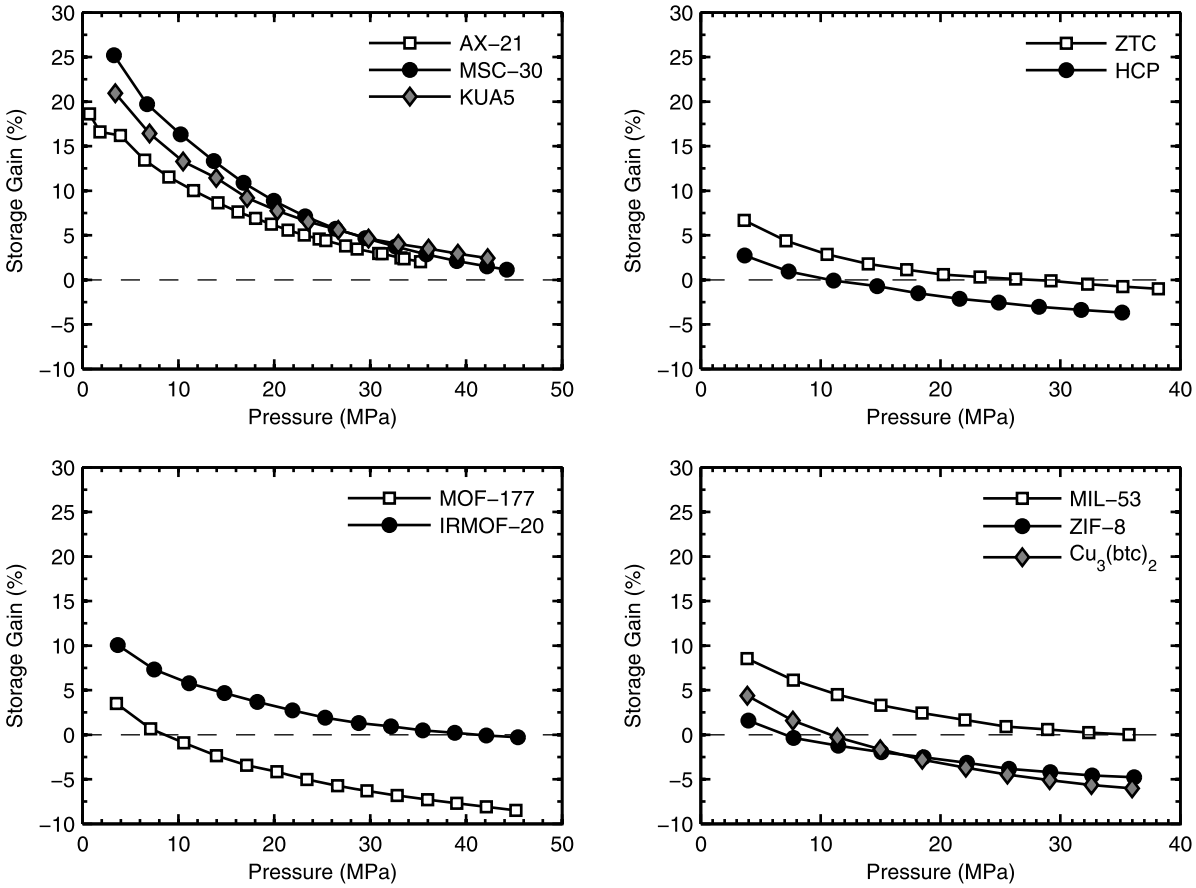

Fig. 4 Volumetric hydrogen storage gain over compressed gas (1) for each material at 298 K

DFT simulations of adsorption on ZIF-8 by Liu et al., who predicted an adsorbed phase density of 19.92 mol L^{-1} at 22.7 MPa (2009). Using an adsorbed monolayer layer thickness of 0.4059 nm from Züttel et al. (2002), the adsorbed phase density measured in this work on ZIF-8 at 298 K is 18 ± 2.0 mol L^{-1} at 22.7 MPa and 25 ± 2.8 mol L^{-1} at 35 MPa. Liu et al. also modeled the adsorbed phase density on MOF-5, an isoreticular MOF based on the ZnO_4 cluster, similar to MOF-177 and IRMOF-20 measured in this study (2009). At 298 K and 30 MPa, their calculated adsorbed density was 11.62 mol L^{-1}, compared with our measurements at 30 MPa of 12.7 ± 0.6 mol L^{-1} and 14.3 ± 0.9 mol L^{-1} on MOF-177 and IRMOF-20, respectively. The difference between these measurements and the modeled values are likely due to differences in the MOF structures, since MOF-5 is built up from a different organic linker and typically has a lower BET surface area than the measured values for the IRMOF-20 and MOF-177 used in this work. Our data provide experimental evidence of the modeled phenomena of higher surface coverage on ZIF-8 compared with isoreticular MOFs.

3.3 Volumetric storage gain

Another way to evaluate adsorbents for hydrogen storage capacity is based on the volumetric storage gain over compressed gas, as described by Bénard and Chahine (2001). This quantity is given in (1) in terms of the bed density (ρ_{bed}), excess adsorption (θ_{excess}), skeletal density (ρ_{sk}), and gas density (ρ_{gas}).

$$Gain\ (\%) = \rho_{bed}\left(\frac{\theta_{excess}}{\rho_{gas}} - \frac{1}{\rho_{sk}}\right) \tag{1}$$

Using the measured skeletal densities from Table 1 and measured bed densities, the storage gains were calculated for each material as a function of pressure (Fig. 4). The bed densities were calculated by dividing the loaded sample volume by the sample mass from Table 1. The loaded sample volume was 2.1 ml for all materials except AX-21 and $Cu_3(btc)_2$, which were tested in a larger 4.6 ml sample holder (the $Cu_3(btc)_2$ did not fill the sample holder and occupied only 4.1 ml). These bed densities varied from 0.12 to 0.3 g ml^{-1} depending on the material.

All of the cases reported are for loosely packed beds of adsorbent, so the magnitude of the storage gain in Fig. 4

could feasibly be increased by a factor of approximately 2–3 by increasing the packing density. However, increased compaction beyond a certain level has been shown to damage the structure and reduce the material's capacity (Zacharia et al. 2010; Bénard and Chahine 2001; Purewal et al. 2012). Additionally, since the bed density does not change the sign of (1), compaction cannot change a negative storage gain to a positive one, so compaction of most of the materials actually results in more negative gains at high pressures. Thus, the point at which the storage gain is zero is an intrinsic material property, independent of the packing density.

For comparison with the storage gains shown above, meeting the 2015 DOE system volumetric hydrogen storage target of 40 $g\,L^{-1}$ at 35 MPa would require a storage gain greater than 70 %. At these elevated pressures, none of the materials examined provides enough storage to produce significant gains over compressed gas. At lower pressures where the storage gains are moderately higher, the required improvement is significantly higher. For example, at 10 MPa a volumetric storage gain greater than 420 % is required to meet the 2015 DOE volumetric target. Reducing the weight of the material's framework may increase its excess adsorption to a level that could approach the DOE gravimetric targets, but such an increase would not necessarily be reflected by any actual volumetric storage increase. A material with a negative volumetric storage gain is merely unused weight added to the storage tank, regardless of its gravimetric hydrogen capacity. Thus, material modifications which improve the volumetric capacity of a potential adsorbent material provide significantly higher benefits in terms of actual storage capacity than modifications which increase gravimetric capacity or specific surface area through reduction of the mass of the adsorbent framework.

3.4 Microstructure effects

Prior studies of adsorbent materials at ambient temperature have primarily focused on the relationship between specific surface area and hydrogen storage capacity. For example, Panella et al. (2005) looked at the hydrogen capacity of a variety of carbon-based nanostructures at 298 K and 6.6 MPa with BET surface areas ranging from 20 to 2560 $m^2\,g^{-1}$ which had not reached saturation and observed a trend of increasing capacity with increasing surface area (2005). On the other hand, Fierro et al. (2010) recently investigated the storage capacity of activated carbon adsorbents with surface areas ranging from approximately 1500 to 2800 $m^2\,g^{-1}$ and did not observe this trend (2010). Rather, the capacity decreased as surface area increased beyond about 2200 $m^2\,g^{-1}$. In both of these studies, hydrogen excess uptakes of metal organic frameworks were not examined, nor had any materials reached saturation. Nonetheless, adsorbent materials are typically evaluated for adsorptive capacity based on their behavior at 77 K, where surface area and micropore volume (<2 nm) are good indicators of potential capacity.

As mentioned previously, our measurements of excess hydrogen uptake at 35 MPa do not show any discernable correlation with the specific surface areas or micropore volumes (<2 nm) of the corresponding materials (Fig. 5). The present data on activated carbons is quite comparable with that of Fierro et al. at 20 MPa, but the inclusion of MOFs in this study widens the range of surface areas and material types considered. It follows that while surface area contributes to total storage, at ambient temperature and high pressures it is not a dominant factor. Relating the excess adsorption at 35 MPa to the specific micropore volume (the volume of pores less than 2 nm) the present data exhibit no discernable relationships either. This is due to the contribution of large pores to the total volume, which varies from material to material and has little effect on the excess adsorption of hydrogen. If we examine the relationship between total pore volume and excess adsorption instead of the micropore volume, a similar lack of a trend is observed, which is expected since the mesopores contribute negligibly to ambient temperature adsorption.

Since common metrics like specific surface area and micropore volume do not correlate with ambient temperature hydrogen uptake, we must consider the physical adsorptive process to explain why certain materials perform better than others. A major factor in determining ambient temperature adsorption capacity is the relative difference between the attractive force of the surface and the thermal energy of the adsorbate. To examine this attractive force we remove the effect of differing surface areas and, following the discussions from Sect. 3.1, focus on the pores which are predicted to have the strongest attractive forces at ambient temperatures (0.6 to 0.9 nm). The effect of the quantity of small pores (less than 0.8 nm) on the measured excess surface coverage at 35 MPa is shown in Fig. 6, where both excess adsorption and the narrow micropore volume have been normalized by the respective material's specific surface area. This normalization allows us to compare differences in hydrogen storage between materials with widely varying surface areas and to observe a more distinct relationship between surface coverage and microporosity than between excess adsorption and specific surface area.

It has been demonstrated in the literature that materials with smaller pores tend to have higher heats of absorption (Schmitz et al. 2008; Gogotsi et al. 2009). In particular, the measurements presented by Schmitz et al. (2008) showed that the small pore size of MIL-53 translated into a higher heat of adsorption. Our measurements at room temperature support this observation, with MIL-53 exhibiting the highest fraction of small pores and the highest excess surface coverage. However, due to its lower surface area its excess adsorption is not significantly higher than most of the other materials considered.

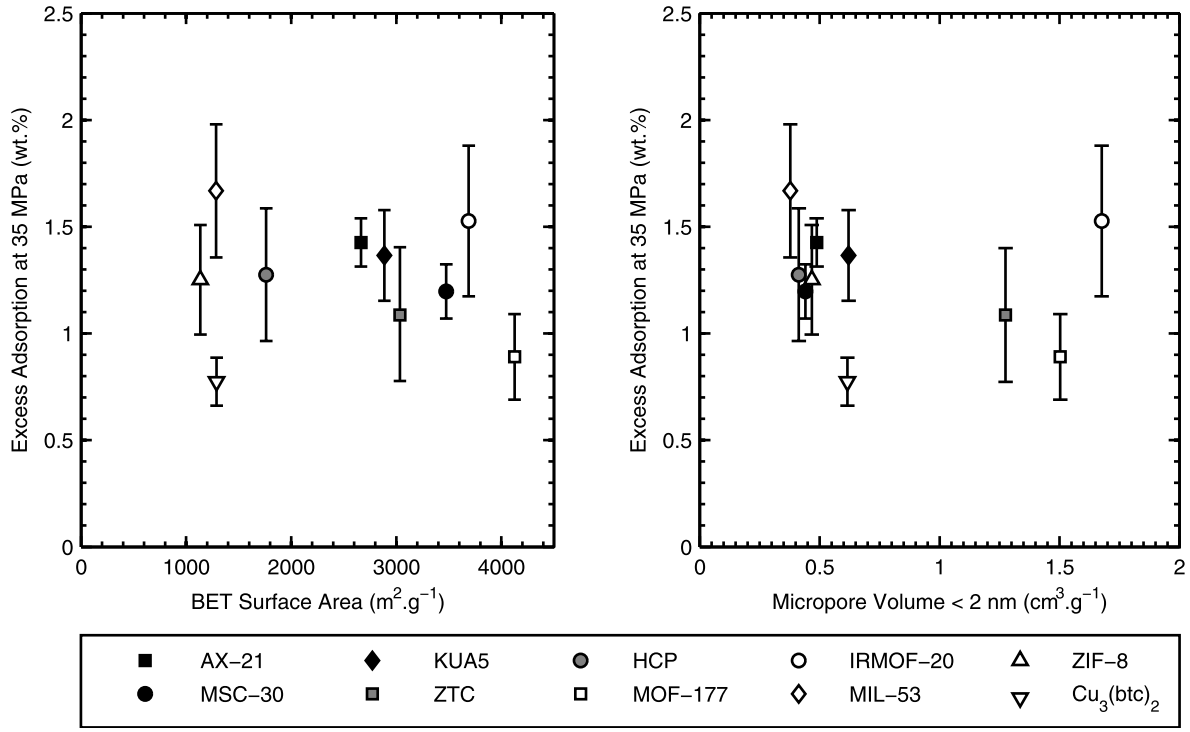

Fig. 5 Excess adsorption of all materials tested at 35 MPa vs. BET specific surface area (*left*) and excess adsorption of all materials tested at 35 MPa vs. micropore volume (<2 nm) (*right*). Note that some materials (AX-21, MSC-30, KUA5, MOF-177) have reached or closely approached saturation while the rest have not

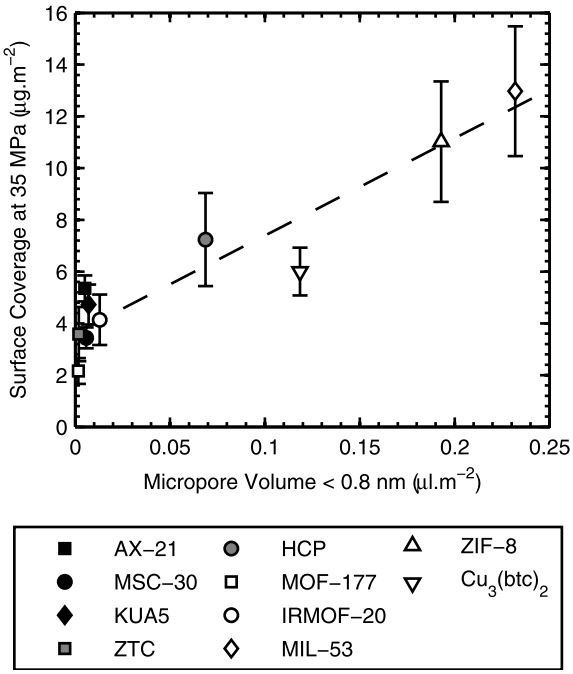

Fig. 6 Comparison of surface coverage and microporosity (below 0.8 nm) normalized by surface area, with a linear fit illustrating the trend of increasing coverage with increasing volumes of sub-nanometer pores

At ambient temperature, significant enhancements to the attractive forces between the hydrogen and the adsorbate which go beyond merely tuning pore sizes are required. Even the materials tested in this study with significant quantities of sub-nanometer pores did not adsorb enough hydrogen to offset the amount of compressed gas they displaced. Doping of microporous adsorbents with metal nanoparticles such as Pt or Ni may increase the hydrogen bond strength with the material through catalytic and spillover mechanisms and improve ambient temperature storage capacities; however this approach has not yet been demonstrated.

4 Conclusions

A set of data including excess isotherms of hydrogen adsorption at 298 K and up to 50 MPa, BET specific surface area, pore size distribution and total pore volume have been obtained on a wide range of microporous materials including activated carbons, zeolite template carbon, hypercrosslinked polymer and Metal Organic Frameworks. By testing these materials at higher pressures than previously reported, we examined the effect of material differences on the excess adsorption beyond the linear Henry's law region that is typically considered at ambient temperatures. The excess hydrogen uptakes at ambient temperatures were related

back to the materials microstructure properties to establish a potential relationship. While a fairly linear trend between the BET specific surface areas and the maximum excess hydrogen uptakes is observed at cryogenic conditions, no such trend was observed at ambient temperatures. The correlation between hydrogen uptake and the total pore volume also observed at 77 K, although with slightly larger scatter, does not hold at 298 K either.

These results are illustrative of the difficulty of predicting hydrogen adsorption at ambient temperatures. Accurate measurements and precise analysis are crucial for determining microporous adsorbents hydrogen storage performance at such conditions. Quantitative predictions of adsorption capacity cannot be directly extrapolated from measurements obtained at cryogenic temperatures. Indeed, one of the most promising materials at cryogenic conditions, MOF-177, adsorbed less hydrogen at ambient temperature than most of the other materials. This observation complements recent DFT studies and provides insight into potential avenues for improvement of adsorption in microporous adsorbents at ambient temperatures.

By considering the volumetric storage gain provided by these materials we showed that despite moderate gravimetric capacities, most of the promising materials actually provided no net volumetric storage gains relative to compressed gas. This highlights the need for a focus not only on the gravimetric capacity of adsorbents, but also on their volumetric capacity, which is by far the most significant factor limiting their feasibility as a solid state gas storage media.

Acknowledgements The authors thank General Motors for their financial support of this project. This manuscript is also based upon work supported under a National Science Foundation Graduate Research Fellowship to the first author. Any opinions, findings, conclusions or recommendations expressed in this publication are those of the author and do not necessarily reflect the views of the National Science Foundation.

Appendix: Uncertainty analysis

The uncertainty in the measured excess adsorption using a volumetric apparatus is a function of the random and bias errors in the experimental measurements (pressure and temperature), the accuracy of the volume calibrations of the system, and the assumptions used in the data analysis (negligible helium adsorption). For the uncertainty analysis presented herein, each instrument was assumed to have its own independent bias error based on manufacturer specifications and random errors were quantified with using the 95 % confidence interval of the time-averaged values.

A.1 Volume calibration

The reservoir volumes in the system were measured with an accuracy of 0.03 ml using the NIST and ASTM volume calibration standards (Bean et al. 2009; ASTM 2007), and the sample chamber void volume was calculated for each test by helium expansion with the sample loaded in the sample chamber with an accuracy of approximately 0.04 ml. Of the typical final uncertainty in excess adsorption (0.1 to 0.4 wt.%, depending on sample mass), approximately 60–70 % of the value is due to uncertainty in the reservoir volume, approximately 5–10 % is due to uncertainty in the sample chamber volume, and the remainder is due to uncertainty in the measured values of pressure and temperature. The large difference between the effects of the two volumes is due to the fact that the mass balance calculation uses the sum of several time periods from the reservoir, but only a single time period from the sample holder to calculate excess adsorption at a given pressure.

A.2 Helium adsorption

The assumption that helium is not adsorbed during the free volume measurements at 298 K is a common assumption often required when using a volumetric apparatus. Its validity, however, has been questioned and discussed in few publications (Sircar 1999, 2001; Lachawiec et al. 2008). The presence of non-zero helium adsorption would result in a constant error in the measurement of the sample chamber's free volume. If the helium expansion is done in the Henry's law region (where the isotherm is linearly proportional to the gas pressure) then this error does not depend on the pressure at which the measurement is taken. In this study, the measurements were all taken at less than 2 MPa, where reported helium isotherms on similar materials are still in the Henry's law region (Hocker et al. 2003). The result of this potential volume error is an under-prediction of the adsorbed amount by an amount which is proportional to the gas density. Thus, for high pressure measurements, this may not be negligible.

Unfortunately, Henry's law constants (K) for helium adsorption on MOFs and other microporous materials are seldom reported in the literature. When reported for carbon adsorbents, they typically vary between 0.01 and 0.1 ml g^{-1} (Sircar 1999, 2001; Lachawiec et al. 2008; Hocker et al. 2003; Springer et al. 1969; Kini and Stacy 1963), although scattered publications have reported values considerably higher and lower than this range. In the worst case, when $K = 0.1$ ml g^{-1}, this results in an error in the excess adsorption of 0.08 wt.%, 0.21 wt.%, and 0.31 wt.% at 10 MPa, 30 MPa, and 50 MPa, respectively. However, if K is 0.01 ml g^{-1} then these errors are also reduced by a factor of 10 and are then negligible compared to other sources of uncertainty in the measurements. Since the error in the sample chamber volume due to helium adsorption is proportional to sample mass, the error in gravimetric capacity (wt.%) is a constant at a given pressure regardless of sample mass.

While it is indeed possible that the effect of helium adsorption is not negligible, it is nonetheless comparable in

magnitude to the other sources of uncertainty outlined previously. Additionally, its measurement typically requires testing at elevated temperatures (600 K) where helium adsorption is very low, which would destroy the structure of most of the MOFs in this study. Since helium adsorption values have not been reported for the majority of the materials tested in this study, we follow the standard procedure of neglecting its effect on the final measurement rather than assume a value and introduce further uncertainty into the reported measurements.

References

Alcañiz-Monge, J., Roman-Martinez, M.C.: Microporous Mesoporous Mater. **112**, 510–520 (2008)

ASTM E 542e01, Standard practice for calibration of laboratory volumetric apparatus (2007)

Bean, V., Espina, P., Wright, J., Houser, J., Sheckels, S., Johnson, A.: NIST calibration services for liquid volume. NIST Special Publication 250-72 (2009)

Bénard, P., Chahine, R.: Int. J. Hydrog. Energy **26**, 849–855 (2001)

Bhatia, S.K., Myers, A.L.: Langmuir **22**, 1688–1700 (2006)

Casa-Lillo, M.A., Lamari-Darkrim, F., Cazorla-Amorós, D., Linares-Solano, A.J.: Phys. Chem. Earth, Part B, Hydrol. Oceans Atmos. **106**, 10930–10934 (2002)

Chen, E.-Y., Liu, Y.-C., Zhou, M., Zhang, L., Wang, Q.: Chem. Eng. Sci. **71**, 178–184 (2012)

Fierro, V., Zhao, W., Izquierdo, M.T., Aylon, E., Celzard, A.: Int. J. Hydrog. Energy **35**, 9038–9048 (2010)

Gogotsi, Y., Portet, C., Osswald, S., Simmons, J.M., Yildirim, T., Laudisio, G., Fischer, J.E.: Int. J. Hydrog. Energy **34**, 6314–6319 (2009)

Gotzias, A., Tylianakis, E., Froudakis, G., Steriotis, T.: Microporous Mesoporous Mater. **154**, 38–44 (2012)

Hocker, T., Rajendran, A., Mazzotti, M.: Langmuir **19**, 1254–1267 (2003)

Im, J.S., Park, S.-J., Kim, T.J., Kim, Y.H., Lee, Y.-S.: J. Colloid Interface Sci. **318**, 42–49 (2008)

Jordá-Beneyto, M., Suárez-García, F., Lozano-Castelló, D., Cazorla-Amorós, D., Linares-Solano, A.: Carbon **45**, 293–303 (2007)

Kini, K.A., Stacy, W.O.: Carbon **1**, 17–24 (1963)

Kowalczyk, P., Tanaka, H., Holyst, R., Kaneko, K., Ohmori, T., Miyamoto, J.: J. Phys. Chem. B **109**, 17174–17183 (2005)

Krkljus, I., Hirscher, M.: Microporous Mesoporous Mater. **142**, 725–729 (2011)

Kumar, K.V., Müller, E.A., Rodríguez-Reinoso, F.: J. Phys. Chem. C **166**, 11820–11829 (2012)

Lachawiec, A.J., DiRaimondo, T.R., Yang, R.T.: Rev. Sci. Instrum. **79**, 63906 (2008)

Leachman, J., Jacobsen, R., Lemmon, E.: J. Phys. Chem. Ref. Data **38**, 721–748 (2009)

Li, Y., Yang, R.T.: Langmuir **23**, 12937–12944 (2007)

Li, Y., Yang, R.T.: AIChE J. **54**, 269–276 (2008)

Liu, Y., Liu, H., Hu, Y., Jiang, J.: J. Phys. Chem. B **113**, 12326–12331 (2009)

Lozanó-Castello, D., Lillo-Rodenas, M.A., Cazorla-Amoros, D., Linares-Solano, A.: Carbon **39**, 741–749 (2001)

Nishihara, H., Hou, P.-X., Li, L.-X., Ito, M., Uchiyama, M., Kaburagi, T., Ikura, A., Katamura, J., Kawarada, T., Mizuuchi, K., Kyotani, T.: J. Phys. Chem. C **113**, 3189–3196 (2009)

Panella, B., Hirscher, M., Roth, S.: Carbon **43**, 2209–2215 (2005)

Panella, B., Hirscher, M., Putter, H., Muller, U.: Adv. Funct. Mater. **16**, 520–524 (2006)

Poirier, E., Dailly, A.: Nanotechnology **20**, 204006 (2009)

Proch, S., Herrmannsdorfer, J., Kempe, R., Kern, C., Jess, A., Seyfarth, L., Senker, J.: Eur. J. Chem. **14**, 8204–8212 (2008)

Purewal, J.J., Liu, D., Yang, J., Sudik, A., Siegel, D.J., Maurer, S., Müller, U.: Int. J. Hydrog. Energy **37**, 2723–2727 (2012). doi:10.1016/j.ijhydene.2011.03.002

Richard, M.-A., Bénard, P., Chahine, R.: Adsorption **15**, 43–51 (2009)

Schmitz, B., Müller, U., Trukhan, N., Schubert, M., Férey, G., Hirscher, M.: ChemPhysChem **9**, 2181–2184 (2008)

Sircar, S.: Ind. Eng. Chem. Res. **38**, 3670–3682 (1999)

Sircar, S.: AIChE J. **47**, 1169–1176 (2001)

Springer, C., Major, C.J., Kammermeyer, K.: J. Chem. Eng. Data **14**, 78–82 (1969)

Sumida, K., Her, J.-H., Dinca, M., Murray, L., Schloss, J., Pierce, C., Thompson, B., FitzGerald, S., Brown, C., Long, J.: J. Phys. Chem. C **115**, 8414–8421 (2011)

Voskuilen, T., Zheng, Y., Pourpoint, T.: Int. J. Hydrog. Energy **35**, 10387–10395 (2010)

Wang, Q., Johnson, J.K.: J. Chem. Phys. **110**, 577–586 (1999)

Wong-Foy, A.G., Matzger, A.J., Yaghi, O.M.: J. Am. Chem. Soc. **128**, 3494–3495 (2006)

Xiong, R., Keffer, D.: Renew. Sustain. Energy Rev. **3**, 053105 (2011)

Zacharia, R., Cossement, D., Lafi, L., Chahine, R.: J. Mater. Chem. **20**, 2145–2151 (2010)

Züttel, A., Sudan, P., Mauron, P., Kiyobayashi, T., Emmenegger, C., Schlapbach, L.: Int. J. Hydrog. Energy **27**, 203–212 (2002)